

Impedans Langmuir Probe and Octiv Poly are used to study the nonlocal electron kinetics and spatial transport in radio-frequency two-chamber inductively coupled argon discharges

INTRODUCTION

Two-chamber inductively coupled plasmas (ICPs) are used in various applications e.g. thin film deposition, synthesis of nanomaterials and neutral beam injection. Depending on the application, a two-chamber ICP source is also called a remote plasma source or a tandem plasma source.

EXPERIMENT

The experimental setup of the two-chamber ICP source driven by cylindrical spiral coils is shown in Figure 1. The upper chamber (driver region) consists of a quartz tube with a 6 cm radius and a length of 14 cm and is surrounded by a 3 turn coil, one side connected to the 13.56 MHz RF power supply through an automatically adjustable π -type matching network while the other side is grounded.

An [Impedans Octiv Poly](#) VI probe is placed between the match box and the power supply to monitor the applied power. The lower chamber (expansion region) is made of stainless steel, with a radius of 15 cm and a length of 40 cm. An [Impedans](#) RF compensated single [Langmuir probe](#) is used to measure the plasma parameters (electron density, effective electron temperature and EEPF). The probe consists of a tungsten wire (diameter 0.1mm, length 5mm) that is mounted either along the axis of the chamber or radially, 6 cm below the interface between the driver and expansion regions.

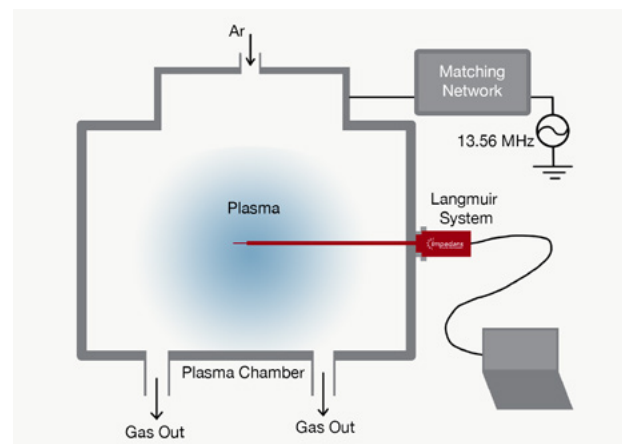


Figure 1. Schematic diagram of the experimental setup.

The working gas, Argon, is fed into the driver region along the axis of the vessel.

FINDINGS AND RESULTS

In Figure 2 the axial distribution of the electron density for a fixed pressure of 1 Pa and power in the range of 500-1000 W is shown. The electron density rises significantly with increasing applied power and exhibits a peak between 6 and 8 cm, which aligns with the coil, with a rapid decrease either side towards the walls. This indicates that the electrons are generated and localised to the driver region. In the expansion region, the electron transport is driven by diffusion from the driver region. Along the axial direction, the effective electron temperature has a slight maximum aligning with the coil centre (6-8 cm) and a gradual decline moving into the expansion region.

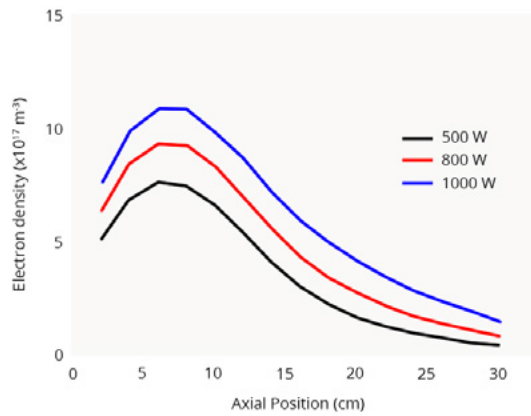


Figure 2. Axial spatial evolution of the electron density at a fixed pressure of 1 Pa for powers ranging from 500- \rightarrow 1000 W.

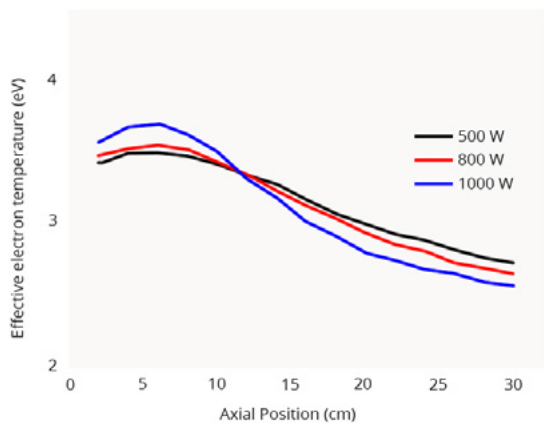


Figure 3. Axial spatial evolution of the effective electron temperature at a fixed pressure of 1 Pa for powers ranging from 500- \rightarrow 1000 W.

The difference between the driver region and the expansion region is small, i.e. less than 1 eV.

Figure 4 shows the EEPFs for select axial positions at a fixed pressure of 1 Pa for varying powers. The EEPFs deviate slightly from a Maxwellian distribution, where the low and middle energy electron groups equalise whereas the high-energy electrons are depleted. The shape of the EEPFs does not significantly change with power, while the increase in power results in a monotonic increase for the entire energy range over the entire volume, i.e. a rise in electron density everywhere due to a strengthening of the RF field in the driver region.

It can be seen in figure 5 that the high energy tail shrinks slightly while the low energy peak increases significantly as the pressure increases. This is due to the higher rate of electron-neutral collisions, which creates more low energy electrons. The slope change occurs in the driver region at the ionisation energy ($\epsilon_i=15.8$ eV) whereas it occurs at the

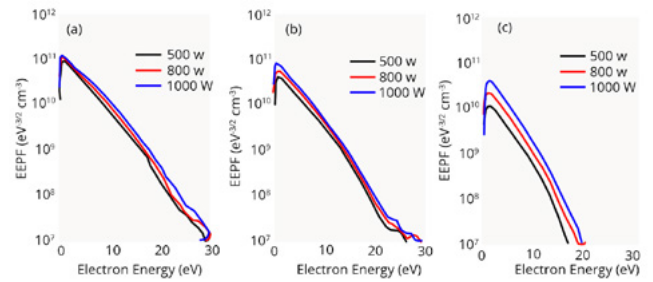


Figure 4. The EEPF vs applied power at the axial positions of (a) 6 cm, (b) 14 cm and (c) 24 cm at 1 Pa.

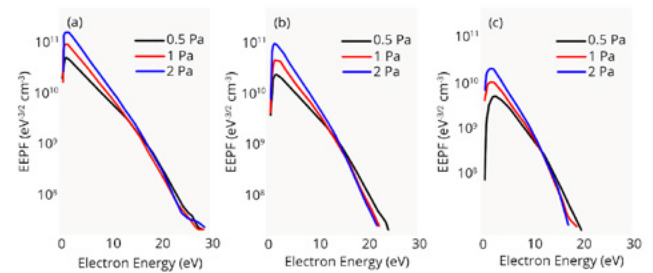


Figure 5. The EEPFs vs pressure at the axial positions of (a) 6 cm, (b) 14 cm and (c) 24 cm at 500 W.

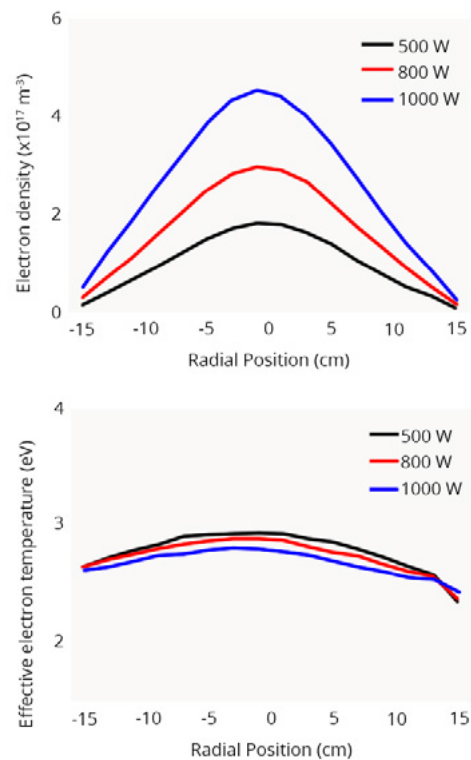


Figure 6. Radial distribution of the electron (a) density and (b) effective temperature for various powers at 1 Pa.

excitation energy ($\epsilon^*=11.55$ eV) in the expansion region. Figures 6 and 7 shows the radial distribution of the electron density and electron effective temperature at various powers and a fixed 1 Pa and at various pressures and a fixed 800 W power respectively at 6 cm (axial position =20 cm) from the interface between the driver and expansion regions. The electron density exhibits a bell shape in both scenarios with the density increasing with both power and pressure as expected.

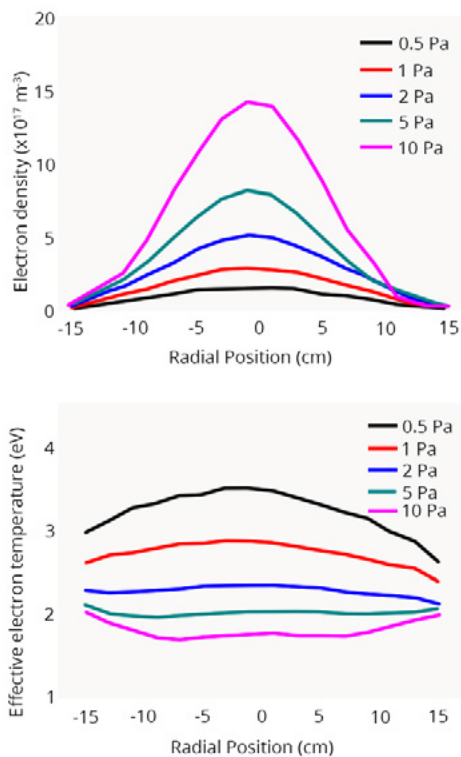


Figure 4. Radial distribution of the electron (a) density and (b) effective temperature for various pressures at 800 W.

The electron temperature decreases slightly as the power increases but drops significantly as the pressure is increased. There is a convex shape as the power is increased. There is no electric field heating in the expansion region causing electrons to gradually lose energy. However, when the pressure is increased the shape transitions from a convex to a concave shape, caused by the increase in electron-electron and electron-neutral collisions, generating an abundance of low energy electrons which are unable to overcome the ambipolar barrier confining them to the axis of the expansion region.

CONCLUSION

The spatial structure and plasma behaviour is characterised in a two-chamber ICP reactor. It is found that the plasma diffusion combined with the nonlocal electron kinetics play an important role, particularly at low pressures.

REFERENCES:

* Li, H. et al, "Nonlocal electron kinetics and spatial transport in radio-frequency two-chamber inductively coupled plasmas with argon discharges" *Journal of Applied Physics*.

Journal of Applied Physics.

Doi: 10.1063/1.4986495

Published in 2017.